

# Spin correlations and velocity-scaling in color-octet NRQCD matrix elements

Geoffrey T. Bodwin,<sup>1</sup> Jungil Lee,<sup>2</sup> and D.K. Sinclair<sup>1</sup>

<sup>1</sup> *High Energy Physics Division, Argonne National Laboratory,*

*9700 South Cass Avenue, Argonne, Illinois 60439*

<sup>2</sup> *Department of Physics, Korea University, Seoul 136-701, Korea*

## Abstract

We compute spin-dependent decay matrix elements for  $S$ -wave charmonium and bottomonium in lattice nonrelativistic quantum chromodynamics (NRQCD). Particular emphasis is placed upon the color-octet matrix elements, since the corresponding production matrix elements are expected to appear in the dominant contributions to the production cross sections at large transverse momenta. We use three slightly different versions of the heavy-quark lattice Green's functions in order to minimize the contributions that scale as powers of the ultraviolet cutoff. The lattice matrix elements that we calculate obey the hierarchy that is suggested by the velocity-scaling rules of NRQCD.

PACS numbers: 13.25.Gv, 12.38.Gc, 13.88.+e, 11.15.Ha

## I. INTRODUCTION

The production rates of the  $J/\psi$  and the  $\Upsilon$  at large transverse momentum ( $p_T$ ) at the Fermilab Tevatron provide important tests of our understanding of heavy-quarkonium systems and of quantum chromodynamics (QCD) itself. The dominant mechanism for both  $J/\psi$  and  $\Upsilon$  production at large  $p_T$  is expected to be the fragmentation of a gluon into a heavy-quark ( $Q\bar{Q}$ ) pair [1, 2]. Because the heavy-quark mass  $m$  provides a large momentum scale, in addition to  $p_T$ , the production of this heavy-quark pair can be calculated perturbatively. The evolution of the  $Q\bar{Q}$  pair into the  $J/\psi$  or the  $\Upsilon$  is a nonperturbative process. In the color-singlet model [3, 4, 5, 6, 7, 8, 9, 10, 11, 12, 13, 14, 15], it is assumed that the  $Q\bar{Q}$  pair is in a color-singlet state. That assumption leads to predictions that are more than an order of magnitude below the Tevatron data [16]. A less *ad hoc* approach to quarkonium production is based on the effective field theory nonrelativistic QCD (NRQCD) [17, 18, 19]. This approach is known as NRQCD factorization. The predictions of NRQCD factorization fit the Tevatron data and indicate that the dominant production mechanism at large  $p_T$  proceeds through the fragmentation of a gluon into a  $Q\bar{Q}$  pair in a color-octet state.

The effective field theory NRQCD separates long-distance, nonperturbative quarkonium dynamics ( $p \lesssim mv$ ) from short-distance, perturbatively calculable processes ( $p \gtrsim m$ ). Here  $m$  is the heavy-quark mass,  $p$  is the magnitude of the relative three-momentum of the  $Q$  and  $\bar{Q}$  in the quarkonium rest frame, and  $v$  is the typical relative velocity of the  $Q$  and  $\bar{Q}$  in the quarkonium rest frame. If  $\Lambda$  is the ultraviolet (UV) cutoff of NRQCD, then physics with  $p < \Lambda \sim m$  is reproduced in the effective field theory, while physics with  $p > \Lambda$  is integrated out, but affects the coefficients of local interactions in the effective theory. The Lagrangian of NRQCD can be expanded in powers of the velocity  $v$ . To any finite order in  $v$  only a limited number of interactions appears in this Lagrangian. Hence, it is useful in calculations for systems in which  $v^2 \ll 1$ . We note that in bottomonium  $v^2 \approx 0.1$ , while in charmonium  $v^2 \approx 0.3$ .

In the context of NRQCD, scaling rules can be deduced for the leading behavior of operator matrix elements in the limit in which the heavy-quark velocity  $v$  approaches zero [19, 20]. When these “ $v$ -scaling rules” are applied to the production of the  $J/\psi$  and the  $\Upsilon$  at large  $p_T$ , they predict that, in the nonperturbative evolution of the  $Q\bar{Q}$  pair into the quarkonium, the non-spin-flip interactions dominate over the spin-flip interactions, with corrections of

order  $v^2$ . Hence, the  $J/\psi$  is predicted to take on most of the transverse polarization of the gluon [21]. However, the CDF data for the polarization [22] show decreasing transverse polarization with increasing  $p_T$  and disagree with the NRQCD prediction [23] in the largest  $p_T$  bin.

The existing calculations of polarization at the Tevatron neglect spin-flip processes in the NRQCD matrix elements, under the assumption that, because of the  $v$ -scaling rules, the spin-flip contributions are relatively suppressed. However, the  $v$ -scaling rules predict only the leading power of  $v$ , not its coefficient. It is usually assumed in making estimates that the coefficients are of order unity, but it could happen that the coefficients of the spin-flip terms are anomalously large or that the coefficients of the non-spin-flip terms are anomalously small. It has also been suggested that the  $v$ -scaling rules themselves may need to be modified in the case of charmonium [24, 25, 26, 27, 28].

One would like to test the applicability of estimates based on the  $v$ -scaling rules by direct calculation of the relevant NRQCD operator matrix elements. At present, lattice QCD is the only technique that is available for calculating color-octet matrix elements. Unfortunately, it is not known how to formulate that calculation of color-octet production matrix elements in Euclidean lattice field theory. However, one does know how to calculate the corresponding decay matrix elements in lattice NRQCD [18, 29, 30]. Since the decay matrix elements are predicted to obey the same velocity-scaling rules as their production counterparts, a test of  $v$ -scaling estimates in the context of decay matrix elements might shed some light on the validity of  $v$ -scaling estimates for production matrix elements. In this paper, we present lattice NRQCD calculations of the decay matrix elements that are related by crossing to those production matrix elements that are expected to dominate  $S$ -wave quarkonium production at large  $p_T$ . Preliminary results of these calculations were presented in Ref. [31].

We use the methods developed by Lepage *et al.* [20] to compute heavy-quark Green's functions in lattice NRQCD. From these, we construct quarkonium propagators and use the methods of Refs. [29, 30] to extract the spin-dependent color-octet matrix elements that contribute to the decays of the  $J/\psi$ ,  $\eta_c$ ,  $\Upsilon$ , and  $\eta_b$  ( $S$ -wave quarkonia) in lattice NRQCD. We perform the lattice measurements on a set of 400  $12^3 \times 24$  quenched configurations at  $\beta = 6/g^2 = 5.7$ . This  $\beta$  value was chosen because it corresponds to a momentum space cutoff  $\Lambda \sim m_b$ . In the case of charmonium one would like to have  $\Lambda \sim m_c$ . However, for

lattices that are significantly coarser than those with  $\beta = 5.7$ , it is not clear, even with highly improved actions, that one is close enough to the continuum limit to make contact with perturbation theory. We therefore use  $\beta = 5.7$  lattices for charmonium and study some of the effects of those contributions that diverge as powers of  $\Lambda/m_c$  by varying the algorithm for calculating lattice heavy-quark Green's functions.

Our bottomonium measurements suggest that the NRQCD  $v$ -scaling rules are useful in determining which matrix elements are most important, and that those contributions that are suppressed as powers of  $v$  show an even greater suppression than one would expect from the  $v$ -scaling factors alone. For charmonium the situation is complicated by our inability to use  $\Lambda \sim m_c$ , but there are indications that the  $v$ -scaling rules are also a good guide here. Calculation of the perturbative coefficients that relate lattice and continuum matrix elements could help to clarify this situation.

In Sec. II we introduce the NRQCD Lagrangian through relative order  $v^4$ , NRQCD factorization of quarkonium production and decay rates, and the lattice implementations of NRQCD that we use. We discuss the calculations that we performed and present our results in Sec. III. Sec. IV contains discussions and our conclusions.

## II. NRQCD

### A. Continuum NRQCD

As we indicated in the Introduction, NRQCD is an effective field theory with a UV momentum-space cutoff  $\Lambda \sim m$ . It is useful in describing bound states of heavy quarks. In the case of  $Q\bar{Q}$  bound states (quarkonium), the terms in the effective Lagrangian can be classified according to their leading power behavior in  $v$ , where  $v$  is the typical heavy-quark (or antiquark) velocity in the quarkonium rest frame [18, 20]. The terms of leading order in  $v^2$  in the NRQCD Lagrangian density are just the Schrödinger Lagrangian density:

$$\mathcal{L}_0 = \psi^\dagger \left( iD_t + \frac{\mathbf{D}^2}{2m} \right) \psi + \chi^\dagger \left( iD_t - \frac{\mathbf{D}^2}{2m} \right) \chi, \quad (1)$$

where  $D_t = \partial_t + igA_0$ ,  $\mathbf{D} = \boldsymbol{\partial} - ig\mathbf{A}$ ,  $\psi$  is the Pauli spinor field that annihilates a heavy quark, and  $\chi$  is the Pauli spinor field that creates a heavy antiquark.

In order to reproduce QCD completely, we would need an infinite number of interactions.

For example, at next-to-leading order in  $v^2$  we have

$$\begin{aligned}
\delta\mathcal{L}_{\text{bilinear}} = & \frac{c_1}{8m^3} [\psi^\dagger(\mathbf{D}^2)^2\psi - \chi^\dagger(\mathbf{D}^2)^2\chi] \\
& + \frac{c_2}{8m^2} [\psi^\dagger(\mathbf{D} \cdot g\mathbf{E} - g\mathbf{E} \cdot \mathbf{D})\psi + \chi^\dagger(\mathbf{D} \cdot g\mathbf{E} - g\mathbf{E} \cdot \mathbf{D})\chi] \\
& + \frac{c_3}{8m^2} [\psi^\dagger(i\mathbf{D} \times g\mathbf{E} - g\mathbf{E} \times i\mathbf{D}) \cdot \boldsymbol{\sigma}\psi + \chi^\dagger(i\mathbf{D} \times g\mathbf{E} - g\mathbf{E} \times i\mathbf{D}) \cdot \boldsymbol{\sigma}\chi] \\
& + \frac{c_4}{2m} [\psi^\dagger(g\mathbf{B} \cdot \boldsymbol{\sigma})\psi - \chi^\dagger(g\mathbf{B} \cdot \boldsymbol{\sigma})\chi].
\end{aligned} \tag{2}$$

In practice, we work to a given precision in  $v$ . For the calculations presented in this paper, the contributions given above suffice.

It has been conjectured that, at large transverse momentum  $p_T$ , the inclusive quarkonium production cross section can be written in a factorized form (Ref. [19]):

$$\sigma(H) = \sum_n \frac{F_n(\Lambda)}{m^{d_n-4}} \langle 0 | \mathcal{O}_n^H(\Lambda) | 0 \rangle. \tag{3}$$

The “short-distance coefficients”  $F_n(\Lambda)$  are essentially the partonic cross sections to make a  $Q\bar{Q}$  pair with a given set of quantum numbers convolved with parton distributions. These partonic cross sections can be calculated as an expansion in  $\alpha_s$ . The  $F_n$  multiply vacuum matrix elements of four-fermion operators of the form

$$\mathcal{O}_n^H = \chi^\dagger \kappa_n \psi \left( \sum_X |H+X\rangle \langle H+X| \right) \psi^\dagger \kappa'_n \chi. \tag{4}$$

$\kappa$  contains Pauli matrices, color matrices, and the covariant derivatives  $D_t = \partial_t + igA_0$ ,  $\mathbf{D} = \boldsymbol{\partial} - ig\mathbf{A}$ .<sup>1</sup> The operator matrix elements contain all of the long-distance, nonperturbative physics and are, essentially, the probabilities for a  $Q\bar{Q}$  pair with a given set of quantum numbers to evolve into a heavy-quarkonium state. The matrix elements are universal, *i.e.*, process independent. NRQCD predicts the leading scaling behavior of the matrix elements with  $v$  (Ref. [19]). As a consequence of these  $v$ -scaling rules, the sum over operator matrix elements can be regarded as an expansion in powers of  $v$ , where  $v^2 \approx 0.3$  for charmonium and  $v^2 \approx 0.1$  for bottomonium.

---

<sup>1</sup> A recent study of certain two-loop contributions to quarkonium production [32] has revealed that, if factorization is to hold, then the matrix elements must be modified from the form given in Eq. (4) by the inclusion of lightlike eikonal lines that run from each of the  $Q\bar{Q}$  bilinears to the far future. It is not known if this modification preserves the factorized form in higher orders.

A similar factorization formula applies to inclusive quarkonium decays [19]:

$$\Gamma(H \rightarrow \text{LH}) = \sum_n \frac{2\text{Im}f_n(\Lambda)}{m_Q^{d_n-4}} \langle H | \mathcal{O}_n(\Lambda) | H \rangle, \quad (5)$$

except that the matrix elements are now between quarkonium states, rather than vacuum states, and the four-fermion operators have the form  $\mathcal{O}_n = \psi^\dagger \kappa_n \chi \chi^\dagger \kappa'_n \psi$ . While the coefficients  $f_n(\Lambda)$  can be calculated perturbatively, the quarkonium matrix elements  $\langle H | \mathcal{O}_n(\Lambda) | H \rangle$  are nonperturbative and can be calculated directly in lattice NRQCD. An important feature of NRQCD factorization is that both quarkonium decay and production occur through color-octet, as well as color-singlet,  $Q\bar{Q}$  states. While the production matrix elements are the crossed versions of quarkonium decay matrix elements, only the color-singlet production and decay matrix elements are simply related.

The NRQCD operator matrix elements in Eqs. (3) and (5) depend explicitly on the cutoff  $\Lambda$ . In the physical decay and production rates, this cutoff dependence in the matrix elements is canceled by a corresponding cutoff dependence in the short-distance coefficients. However, we note that the  $v$ -scaling rules for NRQCD matrix elements are derived under that assumption that the UV cutoff  $\Lambda$  is of order  $mv$ . The matrix elements of NRQCD, in common with those of other effective field theories, contain contributions that diverge, in the limit  $\Lambda \rightarrow \infty$ , both as logarithms and powers of  $\Lambda/m$ . When  $\Lambda$  is larger than  $mv$ , these divergent contributions potentially spoil the  $v$ -scaling rules, with the power divergences being especially important numerically.

As an effective field theory, NRQCD is expected to be valid up to values of  $\Lambda$  close to  $m$  [19, 20]. For bottomonium,  $\Lambda \approx m_b$  is large enough that the physics at momenta greater than  $\Lambda$  can be treated perturbatively. While this choice should not invalidate the  $v$ -scaling rules for UV convergent contributions to matrix elements, it remains to be seen whether the  $v$ -scaling rules remain valid for matrix elements whose leading contributions diverge as  $\Lambda \rightarrow \infty$ . The measurements described in this paper test this conjecture, as well as the  $v$ -scaling rules for  $\Lambda \sim mv$ . In lattice evaluations of the NRQCD matrix elements, the value of the cutoff is determined, in part, by the lattice spacing. As we shall see, the effective cutoff in the matrix elements is also affected by the specific forms of the lattice action and Green's functions that are employed.<sup>2</sup> This latter property allows one to control the effective cutoff in

---

<sup>2</sup> In the continuum phenomenology of quarkonium production, the short-distance coefficients are usually

NRQCD matrix elements without affecting the interactions that determine the quarkonium masses and wave functions. Such an approach is especially useful in the case of charmonium, for which the cutoff  $\Lambda = m_c$  is too small to include all of the nonperturbative bound-state physics.

## B. Lattice NRQCD

The first part of this subsection summarizes the lattice formulation of NRQCD that has been given by Lepage *et al.* [20].

In order to produce a lattice formulation of NRQCD, one must first formulate NRQCD in Euclidean space. This can be accomplished by performing the following substitutions in the NRQCD Lagrangian:

$$\begin{aligned}
t &\rightarrow -it, \\
\partial_t &\rightarrow i\partial_t, \\
D_t &\rightarrow iD_t, \\
\phi &\rightarrow -i\phi, \\
\mathbf{E} &\rightarrow -i\mathbf{E}.
\end{aligned} \tag{6}$$

The gauge fields are incorporated into unitary matrices  $U_\mu(x)$ , which, as usual, are defined on the links of the lattice. Covariant derivatives are replaced on the lattice by covariant finite differences, which are defined by

$$\begin{aligned}
\Delta_i \psi(x) &\equiv \frac{1}{2}[U_i(x)\psi(x+\hat{i}) - U_i^\dagger(x-\hat{i})\psi(x-\hat{i})], \\
\Delta_i^{(2)} \psi(x) &\equiv \frac{1}{2}[U_i(x)\psi(x+\hat{i}) - 2\psi(x) + U_i^\dagger(x-\hat{i})\psi(x-\hat{i})], \\
\Delta^{(2)} &\equiv \sum_i \Delta_i^{(2)}, \\
\Delta^{(4)} &\equiv \sum_i \left(\Delta_i^{(2)}\right)^2.
\end{aligned} \tag{7}$$

---

calculated in dimensional regularization. In dimensional regularization, power infrared divergences in the short-distance coefficients are set to zero. This implies that, in the corresponding continuum NRQCD matrix elements, the UV power-divergent contributions are removed order-by-order in perturbation theory. Therefore, if the lattice matrix elements are to be close in value to the continuum matrix elements, then the effective  $\Lambda$  in the lattice calculations must be of order the heavy-quark mass or less.

Here we have adopted the standard lattice convention of working in a system of units in which the lattice spacing  $a$  has been set to unity.

Tadpole improvement is implemented by making the replacement

$$U_\mu(x) \rightarrow \frac{U_\mu(x)}{u_0}, \quad (8)$$

with  $u_0$  chosen as the fourth root of the average plaquette [33]. For the tadpole-improved action, we expect the perturbation series for quantities at the scale  $\Lambda$  to converge well [33]. Therefore, we replace each of the coefficients  $c_i$  in  $\delta\mathcal{L}_{\text{bilinear}}$  with its lowest-order value, namely, unity.

The order- $v^2$  lattice Hamiltonian is now

$$H_0 = -\frac{\Delta^{(2)}}{2m}. \quad (9)$$

The order- $v^4$  corrections to this Hamiltonian are

$$\begin{aligned} \delta H = & -\frac{(\Delta^{(2)})^2}{8m^3} + \frac{ig}{8m^2}(\mathbf{\Delta} \cdot \mathbf{E} - \mathbf{E} \cdot \mathbf{\Delta}) \\ & -\frac{g}{8m^2}\boldsymbol{\sigma} \cdot (\mathbf{\Delta} \times \mathbf{E} - \mathbf{E} \times \mathbf{\Delta}) - \frac{g}{2m}\boldsymbol{\sigma} \cdot \mathbf{B} \\ & +\frac{\Delta^{(4)}}{24m} - \frac{(\Delta^{(2)})^2}{16nm^2}. \end{aligned} \quad (10)$$

All of the terms except the last two are simple discretizations of those in the continuum expression for  $\delta\mathcal{L}_{\text{bilinear}}$  [Eq. (2)]. The second-to-last term is the order- $a^2$  correction to the discretization of the  $\mathbf{D}^2$  operator in  $H_0$ . The last term is the order- $a^2$  correction to the approximation  $\exp(-H_0) \approx [1 - H_0/(2n)]^{2n}$ , which is used below in computing the evolution of a heavy-quark Green's function over one lattice time step. Here,  $n$  is an integer to be specified below. We note that the form of  $\delta H$  in Eq. (10) is not tadpole-improved correctly by the replacement (8). That is because, in the higher-order derivatives  $\Delta^{(4)}$  and  $(\Delta^{(2)})^2$ , there are canceling factors  $U^\dagger U = 1$  that are, incorrectly, replaced with  $1/u_0^2$ . The corrections to this replacement amount to constant shifts of the Hamiltonian. Nevertheless, we retain the form of  $\delta H$  in Eq. (10), with the replacement (8), because, as noted by the NRQCD collaboration, it makes the contributions from  $\delta H$  to the evolution of the heavy-quark Green's functions small. The smallness of the  $\delta H$  contributions can be discerned from the fact that the spin-averaged “masses” of the quarkonia are little affected by the inclusion of these order- $v^4$  corrections.



We make use of two different forms of the heavy-quark Green's functions, which are equivalent through order  $v^4$ . One is the form that was used in the early spectroscopy papers of the NRQCD collaboration [30, 34]. In this form, for a source  $S(\mathbf{x})\delta_{t,0}$ , the retarded Green's function  $G_r(\mathbf{x}, t)$  at positive time is given recursively by

$$\begin{aligned} G_r(\mathbf{x}, 0) &= S(\mathbf{x})\delta_{t,0}, \\ G_r(\mathbf{x}, 1) &= \left(1 - \frac{H_0}{2n}\right)^n U_4^\dagger \left(1 - \frac{H_0}{2n}\right)^n G_r(\mathbf{x}, 0), \\ G_r(\mathbf{x}, t+1) &= \left(1 - \frac{H_0}{2n}\right)^n U_4^\dagger \left(1 - \frac{H_0}{2n}\right)^n (1 - \delta H) G_r(\mathbf{x}, t). \end{aligned} \quad (11)$$

We call this form of the Green's function the “nrqcd scheme.” A second form of the Green's function is defined for positive time by

$$\begin{aligned} G_r(\mathbf{x}, 0) &= S(\mathbf{x})\delta_{t,0}, \\ G_r(\mathbf{x}, t+1) &= \left(1 - \frac{\delta H}{2}\right) \left(1 - \frac{H_0}{2n}\right)^n U_4^\dagger \left(1 - \frac{H_0}{2n}\right)^n \left(1 - \frac{\delta H}{2}\right) G_r(\mathbf{x}, t). \end{aligned} \quad (12)$$

This second form was used by the NRQCD collaboration in their heavy-light meson calculations [35]. For our calculation, we modify it with the rule that we replace any factor  $(1 - \delta H/2)^2$  that appears as a result of consecutive time-evolution steps with  $(1 - \delta H)$ . This replacement results in an equivalent Green's function to the order in  $v$  to which we work. We implement it because it ensures that the quarkonium spectra of the nrqcd scheme and this second scheme, which we call the “hybrid scheme” are identical. In both the nrqcd and hybrid schemes, we take  $G_r(\mathbf{x}, t) = 0$  for  $t < 0$ . In each scheme, we define a corresponding “advanced” Green's function  $G_a$ , which satisfies the same evolution equations as the hermitian conjugate of  $G_r$ , but with the boundary condition that it vanishes for  $t > 0$ .

We note that the nrqcd and hybrid Green's functions correspond to the same heavy-quark and antiquark propagation, except in the initial and final time slices. The hybrid scheme applies  $\delta H$  to every time slice, including the initial and final time slices. In contrast, the nrqcd scheme does not apply  $\delta H$  to the initial and final time slices, but applies  $\delta H$  to all of the other time slices. In the operator matrix elements that we measure, the four-fermion operator is at the sink of the heavy-quark and antiquark propagators. Hence, in the nrqcd scheme, the interactions in  $\delta H$ , which include those that change the spin, are turned off for one time step on either side of the four-fermion operator.

In order to see the effect of the nrqcd scheme (and related schemes to be described later), let us initially ignore *all* of the interactions of the heavy-quark and antiquark with the gauge

field  $A$ , including those in  $H_0$  and  $U_4$ , in the time step on either side of the four-fermion operator. We call this variant the nrqcdx scheme. In the nrqcdx scheme, the vertices at which  $A$  interacts with the heavy-quark vanish on the time slice that contains the four-fermion vertex. Since this condition is a restriction on the temporal distance between the four-fermion vertex and the nearest heavy-quark-gluon vertex, its effect can be incorporated into the heavy-quark propagator that connects these vertices.<sup>3</sup> One simply sets this propagator to zero at zero temporal separation. Now let us examine how this affects the momentum-space Feynman rule for the propagator. The momentum-space free-field heavy-quark propagator is given by the Fourier transform of the temporal propagator  $\exp[-\mathbf{k}^2 t/(2m)]$ , which has support only for  $t \geq 0$ :

$$\tilde{G}_0(k_0, \mathbf{k}) = \sum_{t=0}^{\infty} e^{\mp i k_0 t} \exp\left(-\frac{\mathbf{k}^2}{2m} t\right). \quad (13)$$

Here  $k$  is the heavy-quark or antiquark momentum, the upper (lower) sign is for the quark (antiquark), and we have approximated the lattice Hamiltonian by the continuum expression. In the nrqcdx scheme, the vanishing of the propagator at zero temporal separation is implemented by removing the  $t = 0$  contribution from the above sum. That is, one replaces a free-field heavy-quark propagator adjacent to the four-fermion vertex with

$$\begin{aligned} \tilde{G}_1(k_0, \mathbf{k}) &= \sum_{t=1}^{\infty} e^{\mp i k_0 t} \exp\left(-\frac{\mathbf{k}^2}{2m} t\right) \\ &= \exp\left(\mp i k_0 - \frac{\mathbf{k}^2}{2m}\right) \tilde{G}_0(k_0, \mathbf{k}). \end{aligned} \quad (14)$$

On the right-hand side of Eq. (14), the oscillatory factor  $\exp(\pm i k_0)$  provides additional damping of the  $k_0$  integration, while the Gaussian factor  $\exp[-\mathbf{k}^2/(2m)]$  cuts off the integration over the spatial components of the momentum at  $|\mathbf{k}| \sim \sqrt{m}$ . In the absence of these factors, the cutoff is of the order of the maximum value of the components of the lattice momentum, *i.e.*,  $\pi$ . In the nrqcdx scheme, the factors in Eq. (14) cut off diagrammatic loops that contain interactions in  $\delta H$ , but only for those loops that involve the four-fermion vertex. We note that these factors appear twice in each loop—once for each of the two heavy-quark propagators in the loop that attach to the four-fermion vertex.

---

<sup>3</sup> Note that additional vertices along the heavy-quark Green's function cannot enter the time slice of the four-fermion interaction because the heavy-quark propagators have a definite time ordering.

As we have mentioned, the NRQCD matrix elements that we measure contain contributions to that grow as powers of the lattice cutoff. These arise in the lowest nontrivial order in perturbation theory from loops involving the four-fermion vertex. Hence, the change in the effective cutoff for such loops that is provided by the nrqcdx scheme helps to control the numerical size of the power-behaved contributions in our simulations. We emphasize that the change in the effective cutoff affects only the interactions that renormalize the four-fermion operator. It has no effect, for example, on the interactions that produce the quarkonium masses or wave functions.

It is useful to examine the effect of the nrqcdx scheme in coordinate space. If the four-fermion operator is at  $t = 0$ , then first interactions after the four-fermion interaction do not occur until  $t = 1$ , at which time the heavy-quark Green's function is just the free-field Green's function

$$G_r(1, \mathbf{x}) = \left(\frac{m}{2\pi}\right)^{3/2} \exp\left(\frac{-mx^2}{2}\right). \quad (15)$$

Hence, in coordinate space, the effect of the nrqcdx scheme is to smear out the four-fermion interaction spatially over a distance of order  $1/\sqrt{m}$ .

Now let us return to the effects of including, in the time slices that are adjacent to the four-fermion interaction, the interactions with the gauge field  $A$  that are contained in  $H_0$  and  $U_4$ . This discussion is relevant to the nrqcd scheme and to the coulomb scheme, which we introduce later. By ignoring the effects of the Coulomb gluon field  $A_0 = \phi$ , we have ignored the effects of the potential in the Schrödinger equation. This is a reasonable approximation until the separation of the  $Q\bar{Q}$  pair is of the order of the typical  $Q\bar{Q}$  separation in the bound state, at which point one can take the spatial smearing to be given roughly by the size of the  $Q\bar{Q}$  bound state. Since we work in the Coulomb gauge, the effects of the heavy-quark interactions with the spatial gauge field  $\mathbf{A}$  are subleading in  $v$  relative to the effects of the potential.

### III. CALCULATIONS AND RESULTS

We are interested in matrix elements between quarkonium states of operators of the form

$$\mathcal{O}_1 (^1S_{0,0}) = \psi^\dagger \chi \chi^\dagger \psi, \quad (16a)$$

$$\mathcal{O}_1 (^3S_{1,\pm 1}) = \psi^\dagger \sigma_\mp \chi \chi^\dagger \sigma_\pm \psi, \quad (16b)$$

$$\mathcal{O}_1 (^3S_{1,0}) = \psi^\dagger \sigma_3 \chi \chi^\dagger \sigma_3 \psi, \quad (16c)$$

and

$$\mathcal{O}_8 (^1S_{0,0}) = \psi^\dagger T^a \chi \chi^\dagger T^a \psi, \quad (17a)$$

$$\mathcal{O}_8 (^3S_{1,\pm 1}) = \psi^\dagger \sigma_\mp T^a \chi \chi^\dagger \sigma_\pm T^a \psi, \quad (17b)$$

$$\mathcal{O}_8 (^3S_{1,0}) = \psi^\dagger \sigma_3 T^a \chi \chi^\dagger \sigma_3 T^a \psi, \quad (17c)$$

where the subscripts 1 and 8 indicate color-singlet and color-octet operators, respectively, and  $S$  denotes an  $S$ -wave operator. In  $^{2s+1}S_{s,m}$ ,  $s$  is the total spin quantum number,  $m$  is the quantum number of the component of the spin along the quantization axis,  $T^a$  is an  $SU(3)$  color matrix in the fundamental representation satisfying  $\text{Tr}(T^a T^b) = (1/2)\delta^{ab}$ , and the  $\sigma$ 's are Pauli spin matrices. In Eqs. (17), there is an implied sum over the color index  $a$ . The matrix elements of the operators in Eqs. (16) and (17) in quarkonium states are those that appear in the NRQCD factorization formula for decays (5). We note that, according to the  $v$ -scaling rules of NRQCD, the matrix elements of the color-octet operators are suppressed by at least  $v^3$  relative to the leading color-singlet matrix elements.

We are interested in the matrix elements of the operators in Eqs. (16,17) between both the spin-singlet (pseudoscalar) and spin-triplet (vector)  $S$ -wave quarkonium states. What we measure is the ratio of octet to singlet matrix elements

$$R(s_i, m_i, s_f, m_f) = \frac{\langle ^{2s_i+1}S_{s_i, m_i} | \mathcal{O}_8 (^{2s_f+1}S_{s_f, m_f}) | ^{2s_i+1}S_{s_i, m_i} \rangle}{\langle ^{2s_i+1}S_{s_i, m_i} | \mathcal{O}_1 (^{2s_i+1}S_{s_i, m_i}) | ^{2s_i+1}S_{s_i, m_i} \rangle_{\text{VS}}}. \quad (18)$$

where the initial (final) spins and  $z$ -components of spin are  $s_i$  ( $s_f$ ) and  $m_i$  ( $m_f$ ), respectively. The subscript VS indicates that we have used the vacuum-saturation approximation [19] for the denominator. That is, we replace the sum over intermediate states in the operator with the vacuum state. We do, in fact, measure the corresponding ratios for the case of color-singlet operators in the numerator, and we find that the spin-diagonal ratios are close to

one, indicating that our use of the vacuum-saturation approximation is valid and that the off-diagonal matrix elements are all small, as is predicted by  $v$  scaling.

Now let us describe how we measure  $R$  on the lattice. First, we create a  $Q\bar{Q}$  pair, using a source on a time slice  $t$ . We propagate this pair to a second time slice  $t' > t$ , using the equations for the retarded Green's functions given in Sec. II. Then we annihilate the  $Q\bar{Q}$  pair at a point, in the spin and color state that corresponds to the operator of interest. We then re-create the  $Q\bar{Q}$  pair at the same point and propagate this pair to time slice  $t'' > t'$ , where it is annihilated at a sink. In practice we use sinks on the time slice  $t''$  as sources and propagate the  $Q\bar{Q}$  pair back to  $t'$  by using the “advanced” Green's functions, conjugating these to give us the Green's functions that we need. We call the quantity that we have just described the “lattice-matrix-element precursor.” For  $T = t' - t$  and  $T' = t'' - t'$  sufficiently large, we annihilate the  $Q\bar{Q}$  pair from an almost pure quarkonium ground-state wave function. The quarkonium propagator falls as  $\exp(-ET)$ , where  $E$  is the energy of this ground state. By computing a ratio of color-octet to color-singlet lattice-matrix-element precursors, we cancel this exponential falloff, as well as the amplitude factors that are associated with the overlaps between the sources and sinks and the quarkonium wave function. The result, in the limit of large  $T$  and  $T'$ , is precisely the lattice version of the ratio  $R$ .

In our calculations, we use one of two stochastic sources on the initial time slice to generate our retarded Green's functions. The first of these sources consists of a complex random number that is uniformly distributed in  $U(1)$  at each site. The second of these sources consists of a Gaussian smearing of this  $U(1)$  random source. By choosing the  $Q$  and  $\bar{Q}$  Green's functions to have conjugate  $U(1)$  sources, we obtain a stochastic estimator of a point source for the  $Q\bar{Q}$  pair at each site on the initial time slice. By choosing the  $U(1)$  source for the  $Q$  and the conjugate of the Gaussian-smeared  $U(1)$  source for the  $\bar{Q}$  (or *vice versa*), we obtain a stochastic estimator of a Gaussian source for the  $Q\bar{Q}$  pair at each site on the initial time slice. The advanced Green's functions are treated similarly.

We calculate the quarkonium propagators and matrix elements on each of 400 equilibrated  $12^3 \times 24$  quenched lattices at  $\beta = 5.7$ . We use the parameters that were determined by the NRQCD collaboration [30, 34, 36]. For  $b$  quarks, we use  $m = 3.15$ , and for  $c$  quarks we use  $m = 0.8$ . We take  $u_0 = 0.860846184$ , which we obtained from our own measurements of the average plaquette. We choose for the width of our Gaussian source 2.5 lattice units, for both charmonium and bottomonium. Fig. 1 shows effective quarkonium “mass” (energy)

plots for point and Gaussian-smeared sources as functions of the time separation  $T$  between the source and the sink. These plots indicate that the Gaussian width that we take is reasonable, as it leads to an early approach to the asymptotic value of the energy. The fits to the effective energy in the nrqcd scheme with the extended source/sink give an  $\eta_c$  energy of  $E_0 = 0.6165(6)$ , with a confidence level of 78% for a fit over the  $T(T')$ -range 8–19, and a  $J/\psi$  energy of  $E_1 = 0.6938(7)$ , with a confidence level of 80% for a fit over the  $T(T')$ -range 10–22. The corresponding fits for bottomonium give an  $\eta_b$  energy of  $E_0 = 0.5065(3)$ , with a confidence level of 60% over the  $T(T')$ -range 8–22, and an  $\Upsilon$  energy of  $E_1 = 0.5215(3)$ , with a confidence level of 59% for a fit over the  $T(T')$ -range 5–22. These results are to be compared with those of the NRQCD collaboration, which obtained  $E_0 = 0.6182(7)$  for the  $\eta_c$ ,  $E_1 = 0.697(1)$  for the  $J/\psi$ ,  $E_0 = 0.5029(5)$  for the  $\eta_b$ , and  $E_1 = 0.5186(6)$  for the  $\Upsilon$ .

Now let us turn to the matrix elements. Here we recall that the decay matrix elements that we measure are related to the production matrix elements that are of primary interest through the crossing of the quarkonium from the intermediate state to the initial state. In the production of the  $J/\psi$  or the  $\Upsilon$  by gluon fragmentation—the dominant process at large  $p_T$ —the gluon fragments into a  $Q\bar{Q}$  pair in a triplet spin state with transverse polarization. Hence, we are most interested in the decay matrix elements in which the annihilated  $Q\bar{Q}$  pair is transversely polarized.

We measure ratios  $R$  of color-octet matrix elements to color-singlet matrix elements defined in Eq. (18). For these measurements we use both the hybrid and the nrqcd schemes for calculating the required heavy-quark Green’s functions.

Let us first examine the bottomonium matrix elements. Here the spin-singlet quarkonium is the  $\eta_b$  and the spin-triplet quarkonium is the  $\Upsilon$ . We fit the measured ratios over a range of  $T$  and  $T'$  values with  $T + T' < 24$  in order to maximize the information that we extract from sometimes noisy “data.” Our measurements are shown in Table I.

The errors presented in Table I are statistical only. For the matrix elements that connect the singlet and triplet spin states and, in the hybrid scheme, for the up  $\rightarrow$  down matrix element, the signal is excellent, and the systematic errors associated with our choices of fits are probably less than the statistical errors. Such estimates of fitting errors are obtained by examining the fits over a number of choices of fitting ranges in  $T$  and  $T'$  (132 choices for each matrix element) and taking into account the range of fitted values and statistical errors for the matrix element of interest. Where possible, we consider only those fits for which

TABLE I: Ratios  $R$  of bottomonium color-octet matrix elements to color-singlet matrix elements, as defined in Eq. (18). The label “singlet” denotes a state  $^1S_{0,0}$ , “triplet” denotes a state  $^3S_{1,m}$ , “up” denotes a state  $^3S_{1,+1}$ , “down” denotes a state  $^3S_{1,-1}$ , and “longitudinal” (long.) denotes a state  $^3S_{1,0}$ . The spin transition  $i \rightarrow f$  is from an initial state  $i$  to an annihilated state  $f$  in the numerator of  $R$ . In the case of triplet states, we average over  $m_i$  in initial states and sum over  $m_f$  in annihilated states. The labels “nrqcd” and “hybrid” refer to the methods for calculating the heavy-quark lattice NRQCD Green’s functions. The column labeled “ $v$  scaling” gives the  $v$ -scaling factors of the various ratios  $R$ , along with their numerical values. In evaluating the  $v$ -scaling factors, we take  $v^2 = 0.1$  for bottomonium.

spin transition	hybrid	nrqcd	$v$ scaling
singlet $\rightarrow$ triplet	$7.169(6) \times 10^{-3}$	$2.72(4) \times 10^{-4}$	$v^3/(2N_c) \approx 5.3 \times 10^{-3}$
triplet $\rightarrow$ singlet	$2.414(3) \times 10^{-3}$	$9.0(1) \times 10^{-5}$	$v^3/(2N_c) \approx 5.3 \times 10^{-3}$
singlet $\rightarrow$ singlet	$6.1(5) \times 10^{-5}$	$6.5(5) \times 10^{-5}$	$v^4/(2N_c) \approx 1.7 \times 10^{-3}$
triplet $\rightarrow$ triplet	$8.1(6) \times 10^{-5}$	$6.9(5) \times 10^{-5}$	$v^4/(2N_c) \approx 1.7 \times 10^{-3}$
up $\rightarrow$ up	$7.3(6) \times 10^{-5}$	$6.9(6) \times 10^{-5}$	$v^4/(2N_c) \approx 1.7 \times 10^{-3}$
long. $\rightarrow$ transverse	$2.7(3) \times 10^{-6}$	$1 - 2 \times 10^{-6}$	$v^6/(2N_c) \approx 1.7 \times 10^{-4}$
down $\rightarrow$ up	$5.53(2) \times 10^{-6}$	$< 5 \times 10^{-8}$	$v^6/(2N_c) \approx 1.7 \times 10^{-4}$

$T$  and  $T'$  are large enough that the value of the matrix element appears to have reached a stable plateau. In the remainder of this paper, when we refer to systematic errors, we mean systematic errors associated with our choices of fits, unless we explicitly state otherwise.

For the three diagonal matrix elements in both schemes, in which the signal is noisy but still substantial, the systematic errors could be as large as 20%. The signal for the longitudinal  $\rightarrow$  transverse matrix element in the hybrid scheme is sufficiently weak that the systematic errors could be as much as 50%. Finally, the signals for the two triplet spin-flip matrix elements in the nrqcd scheme are so noisy that we are only willing to place bounds on their values.

Now let us compare our results with expectations from the  $v$ -scaling rules of NRQCD. The  $v$ -scaling factors of the ratios  $R$  are given in the last column of Table I. For purposes of using the  $v$ -scaling factors to estimate the sizes of matrix elements, we include the color factor  $1/(2N_c)$  that arises in the free  $Q\bar{Q}$  matrix elements, as suggested in Ref. [37]. We

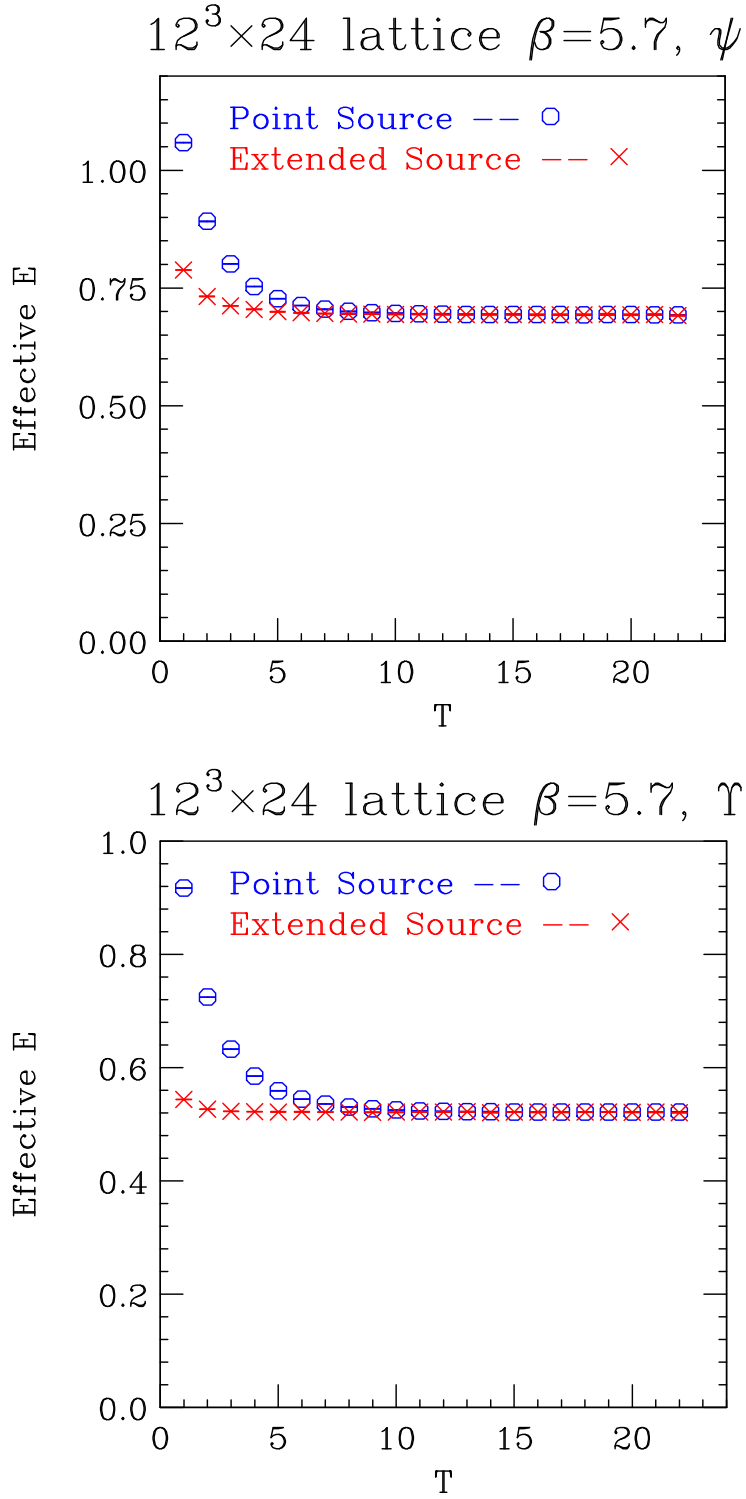


FIG. 1: The effective quarkonium “mass” (energy) as measured with point and Gaussian-smeared (extended) sources for the  $J/\psi$  and the  $\Upsilon$ .  $E$  is the effective energy, and  $T$  is the time separation between the source and the sink. The effective energies shown are measured in the nrqcd updating scheme that is described in Sec. II. The plots in the hybrid scheme and for the  $\eta_c$  and the  $\eta_b$  are similar.



evaluate the  $v$ -scaling factors by taking  $v^2 = 0.1$  for bottomonium. Such  $v$ -scaling estimates are based on the assumption that the coefficients in the expansions of the matrix elements in powers of  $v$  are of order unity. It is that assumption that we wish to test by our explicit calculation. Of course, if it turns out that the coefficients are significantly greater than order unity, then the  $v$  expansion will be of little use.

As we have mentioned, the NRQCD matrix elements that we measure contain contributions that diverge as powers of  $\Lambda$  in the limit  $\Lambda \rightarrow \infty$ . These power-divergent contributions potentially violate the  $v$ -scaling rules, which were derived under the assumption that  $\Lambda$  is of order  $mv$ . For the particular matrix elements that we measure, a perturbative analysis shows that the leading contributions to the singlet  $\rightarrow$  triplet matrix elements diverge as  $[\alpha_s(\Lambda)/\pi](\Lambda/m_b)^2$ , the diagonal contributions diverge as  $[\alpha_s(\Lambda)/\pi]^2(\Lambda/m_b)^2 \log^2(\Lambda/m_b)$ , and the triplet spin-flip contributions diverge as  $[\alpha_s(\Lambda)/\pi]^2(\Lambda/m_b)^4$ . Unless  $\Lambda$  is not much larger than  $mv$ , these power-behaved contributions may lead to significant numerical violations of the  $v$ -scaling rules. As we mentioned earlier, we wish to test not only whether the  $v$ -scaling rules hold for cutoffs  $\Lambda \sim m_b v$ , but also whether they continue to hold for cutoffs  $\Lambda \sim m_b$ . Therefore, in testing the  $v$ -scaling rules in the bottomonium system, we choose  $\Lambda/m_b \sim 1$ . As we stated earlier, at  $\beta = 5.7$ , the lattice momentum cutoff itself is close to the input  $b$ -quark mass. Hence, in the case of bottomonium, no special choice of heavy-quark Green's functions is required in order to control power-behaved contributions, and we focus on the hybrid scheme.

In the hybrid scheme, we note that the singlet  $\rightarrow$  triplet matrix elements are the largest color-octet matrix elements, as is predicted by the  $v$ -scaling estimates. The  $v$ -scaling estimates also predict their magnitudes correctly. The heavy-quark spin symmetry of NRQCD predicts that the singlet  $\rightarrow$  triplet matrix element should be a factor 3 larger than the triplet  $\rightarrow$  singlet matrix element, with corrections to that relation of order  $v^2$ . This prediction is borne out by our measurements. The diagonal matrix elements are suppressed relative to the singlet  $\rightarrow$  triplet and triplet  $\rightarrow$  singlet matrix elements, as expected, but by considerably more than would be expected from the  $v$ -scaling factors alone, suggesting that their coefficients in the  $v$  expansion are small. The triplet spin-flip matrix elements are smaller still, as is expected from the  $v$ -scaling estimates, but, again, they are much smaller than would be expected from the  $v$ -scaling factors alone. The suppression of the triplet spin-flip matrix elements relative to the diagonal matrix elements is approximately what

would be expected from the  $v$ -scaling factors.

The effects of a change in the effective cutoff  $\Lambda$  can be seen when we compare the hybrid-scheme and nrqcd-scheme values for  $R$  in Table I. The nrqcd scheme results in a smaller effective cutoff for the interactions in  $\delta H$ , which include all of the spin-dependent interactions. We see that the nrqcd-scheme singlet  $\rightarrow$  triplet and triplet  $\rightarrow$  singlet matrix elements are suppressed by a factor of about 26 relative to the corresponding hybrid-scheme matrix elements. The triplet spin-flip matrix elements also appear to be suppressed. The diagonal matrix elements are virtually unchanged. That is expected because the leading contribution to the diagonal matrix elements comes from  $H_0$ , whose effective cutoff is not changed in going from the hybrid scheme to the nrqcd scheme.

Now let us turn to the charmonium case. For charmonium, the heavy-quark mass in lattice units is only 0.8, while, as usual, the components of the lattice momentum can range up to  $\pi$  in magnitude. Hence, we expect that the lowering of the effective cutoff  $\Lambda$  that is provided by using the nrqcd scheme will be helpful in reducing the effects of the power-behaved contributions. In the case of charmonium, we will also consider an additional scheme for computing the heavy-quark Green's functions in which the links  $U_i(x)$  are set to unity on the time slice that is associated with the four-fermion operator (the time slice in which the  $Q\bar{Q}$  pair is annihilated and re-created). In other respects, this scheme, which we call the “coulomb scheme” is identical to the nrqcd scheme. In the coulomb scheme, we are neglecting the interactions of the heavy quark with the fields  $A_i$  on the  $Q\bar{Q}$ -annihilation time slice. Since we work in the Coulomb gauge, these interactions are subleading in  $v^2$ . The effect of the coulomb scheme, relative to the nrqcd scheme, is to lower the effective cutoff on  $H_0$  so that it is the same as the effective cutoff on  $\delta H$ . Hence, we expect the diagonal matrix elements to show the effects of a reduced cutoff.

The values of  $R$  in the hybrid, nrqcd, and coulomb schemes, along with the  $v$ -scaling factors, are given in Table II. Again, the quoted errors are statistical only. In the hybrid scheme, the signal for the triplet  $\rightarrow$  singlet, singlet  $\rightarrow$  triplet, and up  $\rightarrow$  down matrix elements is robust, and we feel confident that the systematic errors are less than the statistical errors. The signal for the singlet  $\rightarrow$  singlet matrix element is noisier, but still quite good, so that we feel that the systematic error is probably no worse than the statistical error. The signals for the up  $\rightarrow$  up and transverse  $\rightarrow$  longitudinal matrix elements are even noisier, but still substantial. In these cases, the systematic errors might be as large as 10%. In the

TABLE II: Ratios  $R$  of charmonium color-octet matrix elements to color-singlet matrix elements, as defined in Eq. (18). The labels are as in Table I, except that “coulomb” refers to an additional method for calculating the heavy-quark lattice NRQCD Green’s functions, as described in the text. For purposes of numerical estimates of the  $v$ -scaling factors, we take  $v^2 = 0.3$  for charmonium.

spin transition	hybrid	nrqcd	coulomb	$v$ scaling
singlet $\rightarrow$ triplet	$6.397(8) \times 10^{-2}$	$2.90(3) \times 10^{-3}$	$2.84(4) \times 10^{-3}$	$v^3/(2N_c) \approx 2.7 \times 10^{-2}$
triplet $\rightarrow$ singlet	$2.938(7) \times 10^{-2}$	$1.13(2) \times 10^{-3}$	$1.06(1) \times 10^{-3}$	$v^3/(2N_c) \approx 2.7 \times 10^{-2}$
singlet $\rightarrow$ singlet	$5.03(9) \times 10^{-4}$	$9.7(2) \times 10^{-4}$	$3.6(3) \times 10^{-4}$	$v^4/(2N_c) \approx 1.5 \times 10^{-2}$
triplet $\rightarrow$ triplet	$1.57(2) \times 10^{-3}$	$1.016(8) \times 10^{-3}$	$4.0(4) \times 10^{-4}$	$v^4/(2N_c) \approx 1.5 \times 10^{-2}$
up $\rightarrow$ up	$4.57(6) \times 10^{-4}$	$1.019(8) \times 10^{-3}$	$3.9(4) \times 10^{-4}$	$v^4/(2N_c) \approx 1.5 \times 10^{-2}$
long. $\rightarrow$ transverse	$2.82(4) \times 10^{-4}$	$2.8(7) \times 10^{-6}$	—	$v^6/(2N_c) \approx 4.5 \times 10^{-3}$
down $\rightarrow$ up	$8.48(5) \times 10^{-4}$	$1.4(2) \times 10^{-6}$	$1.4(3) \times 10^{-6}$	$v^6/(2N_c) \approx 4.5 \times 10^{-3}$

nrqcd scheme, the signals for the triplet  $\rightarrow$  singlet, singlet  $\rightarrow$  triplet, and singlet  $\rightarrow$  singlet matrix elements are as clean as those in the hybrid scheme. The signals for the two diagonal triplet matrix elements show some rise as  $T$  and  $T'$  are increased, and the systematic error could be as large as 10%. The signals for the two triplet spin-flip matrix elements are so noisy that the values given should be considered only to be order-of-magnitude estimates. In the coulomb scheme, the signals for all of the matrix elements are noisier than in either of the other two schemes. The triplet  $\rightarrow$  singlet and singlet  $\rightarrow$  triplet elements probably have systematic errors that are comparable with their statistical errors. The diagonal matrix elements could have systematic errors as large as 20%, while the signals for the triplet spin-flip matrix elements are so noisy that we can only say that these matrix elements are small. In Figure 2 we show examples of the signals for the charmonium ratios  $R$  as functions of  $T = T'$ . The upper plot shows  $R$  for the singlet  $\rightarrow$  triplet transition in the hybrid scheme, which has one of the clearest signals that we have seen. The lower plot shows  $R$  for the longitudinal  $\rightarrow$  transverse transition in the coulomb scheme, which has one of the noisiest signals that we have seen.

Now let us compare these results with the predictions from the  $v$ -scaling factors, which are shown in the last column of Table II. As in the bottomonium case, we include the color factor  $1/(2N_c)$  that arises in the free  $Q\bar{Q}$  matrix elements (Ref. [37]). The charmonium  $v$ -scaling

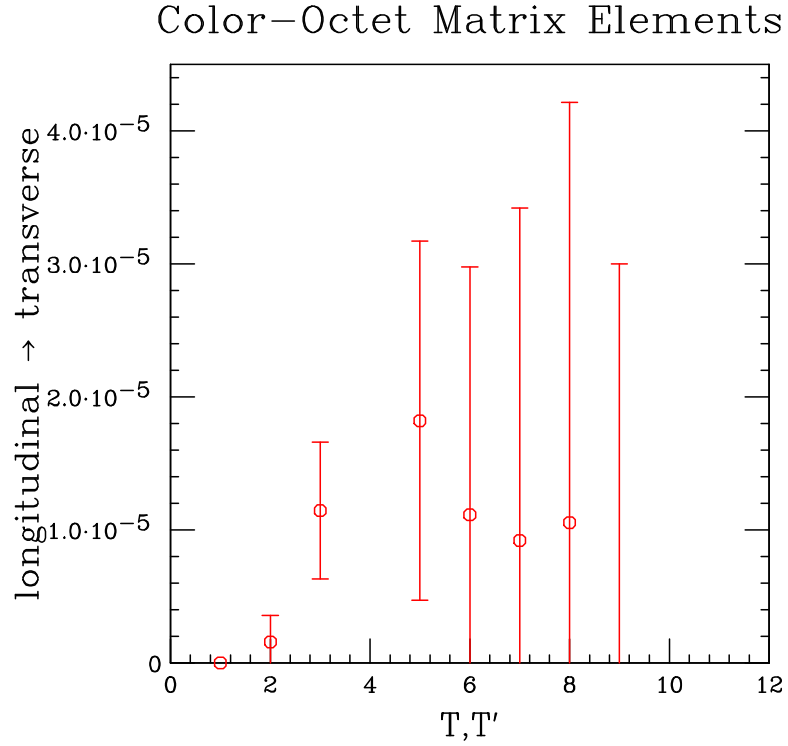
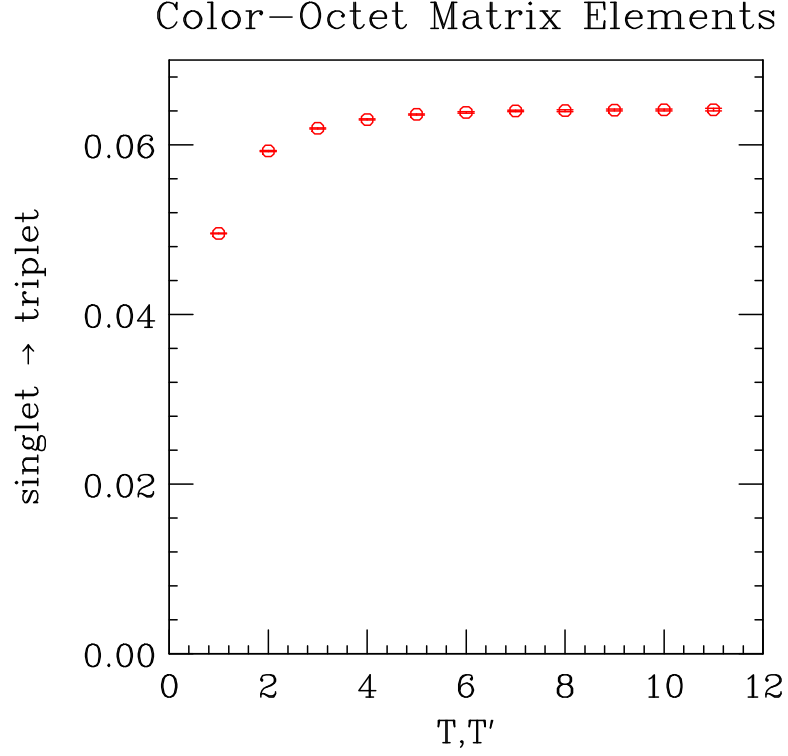


FIG. 2: Values of ratios  $R$  for charmonium as a function of  $T = T'$ . The upper plot shows  $R$  for the singlet  $\rightarrow$  triplet spin transition in the hybrid scheme. The lower plot shows  $R$  for the longitudinal  $\rightarrow$  transverse spin transition in the coulomb scheme.

factors are the same as those for bottomonium, except that we evaluate them by setting  $v^2 = 0.3$ . Again, as in the case of bottomonium, the triplet  $\rightarrow$  singlet and singlet  $\rightarrow$  triplet matrix elements in the hybrid scheme show good agreement with the  $v$ -scaling predictions. The other matrix elements are somewhat smaller than would be expected from the  $v$ -scaling predictions, perhaps indicating that their coefficients in the  $v$  expansion are small. However, here we notice that the triplet spin-flip and non-spin-flip matrix elements are of similar size. As we have mentioned, we know that the effective cutoff in the charmonium case is larger than  $m$  and that the spin-flip matrix elements diverge as  $[\alpha_s(\Lambda)/\pi]^2(\Lambda/m_c)^4$  at large  $\Lambda$ , while the non-spin-flip matrix elements diverge only as  $[\alpha_s(\Lambda)/\pi]^2(\Lambda/m_c)^2 \log^2(\Lambda/m_c)$ . Therefore, it is not surprising that the triplet spin-flip matrix elements appear to be anomalously large in comparison with the non-spin-flip matrix elements. In the nrqcd scheme, which effectively lowers the cutoff on the interactions in  $\delta H$ , we see a considerable reduction in the size of the triplet spin-flip matrix elements, as well as in the triplet  $\rightarrow$  singlet and singlet  $\rightarrow$  triplet matrix elements, which diverge as  $[\alpha_s(\Lambda)/\pi](\Lambda/m_c)^2$ . However, the sizes of the diagonal matrix elements are not reduced, but merely made closer in value, as would be expected when all off-diagonal matrix elements are small. This indicates that these diagonal matrix elements get sizable contributions from the interactions in  $H_0$ , whose effective cutoff is not reduced in the nrqcd scheme. In the coulomb scheme, in which the effective cutoff of the interactions in  $H_0$  is also reduced, we see that the diagonal matrix elements are reduced in size relative to those in the nrqcd scheme. The triplet  $\rightarrow$  singlet and singlet  $\rightarrow$  triplet matrix elements are almost identical in size to their nrqcd-scheme counterparts because the effective cutoff on the interactions in  $\delta H$  is the same (to leading order in  $v$ ) in both schemes. In addition, to the extent that we can infer anything from the very noisy signals for the triplet spin-flip matrix elements in the coulomb scheme, the values of these matrix elements are consistent with their remaining unchanged in going from the nrqcd scheme to the coulomb scheme. We can therefore conclude that, were we able to carry out the lattice computation directly at  $\Lambda \sim m_c$ , the size ordering of matrix elements would be as predicted by the  $v$ -scaling estimates. However, the suppression of the matrix elements of higher order in  $v$  would be even more than that which is predicted by those estimates, indicating that those matrix elements have relatively small coefficients in the  $v$  expansion. We conclude that the  $v$  expansion is a useful tool for establishing a hierarchy of charmonium decay matrix elements.

## IV. SUMMARY AND CONCLUSIONS

We have calculated, in lattice NRQCD, color-octet, spin-dependent matrix elements that appear in the NRQCD factorization expression (5) for decays of bottomonium and charmonium. The lattice action we used is correct through order  $v^4$  and contains the standard tadpole improvement, as well as order- $a^2$  improvements to the terms of leading order in  $v$ . The decay matrix elements that we calculated are related by crossing symmetry to the production matrix elements that appear in the dominant contributions at large  $p_T$  to the production of the  $\Upsilon$  and the  $J/\psi$ . In our calculations, we made use of various forms of the lattice heavy-quark Green's functions, which are equivalent to the order in  $v$  to which we work, but which allow us to vary the effective momentum cutoff for interactions of the heavy-quark fields with the gauge fields. Our goals were to test the accuracy of estimates of the sizes of matrix elements that are based on the  $v$ -scaling rules of NRQCD and to test the convergence of the  $v$  expansion.

In the case of bottomonium, we found that estimates that are based on the  $v$ -scaling factors are reasonable for the singlet  $\rightarrow$  triplet and triplet  $\rightarrow$  singlet matrix elements. The diagonal singlet  $\rightarrow$  singlet and triplet  $\rightarrow$  triplet matrix elements are suppressed relative to these leading-order matrix elements, but by even more than one would expect from the  $v$ -scaling factors alone. The suppression of the triplet spin-flip matrix elements relative to the triplet non-spin-flip matrix elements is consistent with predictions that are based on the  $v$ -scaling factors. In all cases, the  $v$ -scaling predictions correctly indicate the hierarchy of matrix elements.

In the case of charmonium, the situation is made less clear by the fact that, in order to describe the quarkonium physics on the lattice, we are forced to work with lattice spacings that correspond to UV momentum cutoffs that are considerably larger than the heavy-quark mass. Consequently, we expect the matrix-element calculations to contain large contributions that grow as a power of the cutoff and that violate the  $v$ -scaling rules of NRQCD. By using various forms of the heavy-quark Green's functions, we are able to vary the effective UV cutoffs of the matrix elements. The indications from our studies of the effects of varying these cutoffs are that the  $v$ -scaling rules are a good guide as to which matrix elements are important, but that the matrix elements are smaller than one would expect from the  $v$ -scaling factors alone. Again, the  $v$ -scaling predictions correctly indicate the hierarchy of matrix

elements. Of course, the cutoff dependences of the matrix elements are canceled in physical quantities, such as the quarkonium production and decay rates, by corresponding cutoff dependences in the accompanying short-distance coefficients. A more complete understanding of the effects of varying the UV cutoffs could be obtained by studying the cutoff dependences of the matrix elements in perturbation theory. For example, one could calculate the matching coefficients between lattice matrix elements and continuum (dimensionally-regulated) matrix elements. The matching coefficients are infrared safe and, hence, are amenable to a perturbative treatment. Such a calculation involves both one- and two-loop contributions in lattice and continuum perturbation theory, and is beyond the scope of this paper.

Phenomenological color-octet production matrix elements for the triplet  $\rightarrow$  triplet transition, normalized against the color-singlet matrix elements, as in  $R$  in Tables I and II, lie in the ranges  $5.1\text{--}16 \times 10^{-3}$  for the  $\Upsilon(1S)$  and  $1.9\text{--}24 \times 10^{-3}$  for the  $J/\psi$  (Ref. [38]). The lattice decay matrix elements for the triplet  $\rightarrow$  triplet transition are somewhat smaller than the phenomenological range of production matrix elements for the  $J/\psi$  and considerably smaller than the phenomenological range of production matrix elements for the  $\Upsilon$ . However, effects from multiple-gluon radiation, which may decrease the phenomenological values of the color-octet matrix elements, have not yet been included in the analyses of the  $\Upsilon$  matrix elements. Furthermore, decay matrix elements need not be equal to the corresponding production matrix elements, even though they have the same  $v$ -scaling behavior. We also note that lattice matrix elements differ from continuum matrix elements. We do not expect the differences to be large for tadpole-improved lattice calculations, provided that the lattice cutoff is of order or smaller than the heavy-quark mass. However, that situation does not hold in our charmonium calculations.

The charmonium color-octet singlet  $\rightarrow$  triplet decay matrix element is relatively large, which suggests that the color-octet triplet  $\rightarrow$  singlet production matrix element may also be large. This would imply that, at large  $p_T$  at the Tevatron, where the color-octet, spin-triplet process dominates  $S$ -wave quarkonium production, the  $\eta_c$  production rate may be comparable to the  $J/\psi$  production rate. Once the size of the effective UV cutoff is reduced, the longitudinal  $\rightarrow$  transverse decay matrix element is small relative to the up  $\rightarrow$  up decay matrix element. This suggests that a similar hierarchy may hold for the transverse  $\rightarrow$  longitudinal and up  $\rightarrow$  up production matrix elements, which would support the prediction of large transverse polarization at large  $p_T$  at the Tevatron.

## Acknowledgments

We would like to thank Christine Davies, Peter Lepage, and Junko Shigemitsu for helpful discussions on lattice NRQCD. JL thanks the Argonne Theory Group for its hospitality. GTB and DKS are supported by the US Department of Energy under contract W-31-109-ENG-38. JL is supported by a Korea Research Foundation Grant (KRF-2004-015-C00092).

- 
- [1] E. Braaten and T. C. Yuan, Phys. Rev. Lett. **71**, 1673 (1993) [arXiv:hep-ph/9303205].
  - [2] E. Braaten and T. C. Yuan, Phys. Rev. D **52**, 6627 (1995) [arXiv:hep-ph/9507398].
  - [3] M. B. Einhorn and S. D. Ellis, Phys. Rev. D **12**, 2007 (1975).
  - [4] S. D. Ellis, M. B. Einhorn, and C. Quigg, Phys. Rev. Lett. **36**, 1263 (1976).
  - [5] C. E. Carlson and R. Suaya, Phys. Rev. D **14**, 3115 (1976).
  - [6] J. H. Kühn, Phys. Lett. B **89**, 385 (1980).
  - [7] T. A. DeGrand and D. Toussaint, Phys. Lett. B **89**, 256 (1980).
  - [8] J. H. Kühn, S. Nussinov, and R. Rückl, Z. Phys. C **5**, 117 (1980) .
  - [9] M. B. Wise, Phys. Lett. B **89**, 229 (1980).
  - [10] C.-H. Chang, Nucl. Phys. B **172**, 425 (1980).
  - [11] E. L. Berger and D. L. Jones, Phys. Rev. D **23**, 1521 (1981).
  - [12] R. Baier and R. Rückl, Nucl. Phys. B **201**, 1 (1982).
  - [13] R. Baier and R. Rückl, Phys. Lett. B **102** (1981) 364.
  - [14] W. Y. Keung, Print-81-0161 (BNL) *Presented at Z0 Physics Workshop, Ithaca, N.Y., Feb 6-8, 1981*.
  - [15] R. Baier and R. Rückl, Z. Phys. C **19** (1983) 251.
  - [16] See N. Brambilla *et al.*, arXiv:hep-ph/0412158. and references therein.
  - [17] W. E. Caswell and G. P. Lepage, Phys. Lett. B **167**, 437 (1986).
  - [18] B. A. Thacker and G. P. Lepage, Phys. Rev. D **43**, 196 (1991).
  - [19] G. T. Bodwin, E. Braaten, and G. P. Lepage, Phys. Rev. D **51**, 1125 (1995) [Erratum-ibid. D **55**, 5853 (1997)] [arXiv:hep-ph/9407339].
  - [20] G. P. Lepage, L. Magnea, C. Nakhleh, U. Magnea, and K. Hornbostel, Phys. Rev. D **46**, 4052 (1992) [arXiv:hep-lat/9205007].



- [21] P. L. Cho and M. B. Wise, Phys. Lett. B **346**, 129 (1995) [hep-ph/9411303].
- [22] T. Affolder *et al.* [CDF Collaboration], Phys. Rev. Lett. **85**, 2886 (2000) [hep-ex/0004027].
- [23] E. Braaten, B. A. Kniehl, and J. Lee, Phys. Rev. D **62**, 094005 (2000) [hep-ph/9911436].
- [24] M. Beneke, [hep-ph/9703429].
- [25] N. Brambilla, A. Pineda, J. Soto, and A. Vairo, Nucl. Phys. B **566**, 275 (2000) [hep-ph/9907240].
- [26] S. Fleming, I. Z. Rothstein, and A. K. Leibovich, Phys. Rev. D **64**, 036002 (2001) [hep-ph/0012062].
- [27] M. A. Sanchis-Lozano, Int. J. Mod. Phys. A **16**, 4189 (2001) [hep-ph/0103140].
- [28] N. Brambilla, D. Eiras, A. Pineda, J. Soto, and A. Vairo, Phys. Rev. D **67**, 034018 (2003) [hep-ph/0208019].
- [29] G. T. Bodwin, S. Kim, and D. K. Sinclair, Nucl. Phys. B (Proc. Suppl.) **34**, 434 (1994); **42**, 306 (1995) [hep-lat/9412011]; G. T. Bodwin, D. K. Sinclair, and S. Kim, Phys. Rev. Lett. **77**, 2376 (1996) [hep-lat/9605023]; Int. J. Mod. Phys. A **12**, 4019 (1997) [hep-ph/9609371]; Phys. Rev. D **65**, 054504 (2002) [hep-lat/0107011].
- [30] C. T. H. Davies, K. Hornbostel, A. Langnau, G. P. Lepage, A. Lidsey, J. Shigemitsu, and J. H. Sloan, Phys. Rev. D **50**, 6963 (1994) [arXiv:hep-lat/9406017].
- [31] G. T. Bodwin, J. Lee, and D. K. Sinclair, in *Quark Confinement and the Hadron Spectrum V*, AIP Conf. Proc. No. 756 (AIP, New York, 2005) [arXiv:hep-lat/0412006].
- [32] G. C. Nayak, J. W. Qiu, and G. Sterman, Phys. Lett. B **613**, 45 (2005) [arXiv:hep-ph/0501235].
- [33] G. P. Lepage and P. B. Mackenzie, Phys. Rev. D **48**, 2250 (1993) [arXiv:hep-lat/9209022].
- [34] C. T. H. Davies, K. Hornbostel, G. P. Lepage, A. J. Lidsey, J. Shigemitsu and, J. H. Sloan, Phys. Rev. D **52**, 6519 (1995) [arXiv:hep-lat/9506026].
- [35] S. Collins, C. T. H. Davies, J. Hein, G. P. Lepage, C. J. Morningstar, J. Shigemitsu, and J. H. Sloan, Phys. Rev. D **63**, 034505 (2001) [arXiv:hep-lat/0007016].
- [36] C. T. H. Davies, K. Hornbostel, G. P. Lepage, A. Lidsey, P. McCallum, J. Shigemitsu, and J. H. Sloan [UKQCD Collaboration], Phys. Rev. D **58**, 054505 (1998) [arXiv:hep-lat/9802024].
- [37] A. Petrelli, M. Cacciari, M. Greco, F. Maltoni, and M. L. Mangano, Nucl. Phys. B **514**, 245 (1998) [arXiv:hep-ph/9707223].
- [38] M. Kramer, Prog. Part. Nucl. Phys. **47**, 141 (2001) [arXiv:hep-ph/0106120].